



Ezetimibe attenuates functional impairment via inhibition of oxidative stress and inflammation in traumatic spinal cord injury

Wei Rong¹, Huimin Li¹, Huadong Yang¹, Bei Yuan¹, Jianjin Zhu¹, Jiuzheng Deng¹, Songhua Xiao¹, Cheng Zhang^{2*}

¹ Department of Orthopedics, Beijing Tsinghua Changgung Hospital Medical Center, Tsinghua University, Beijing, China

² Beijing Key Laboratory of Bioelectromagnetism, Institute of Electrical Engineering, Chinese Academy of Sciences, Beijing, China

ARTICLE INFO

Original paper

Article history:

Received: March 12, 2023

Accepted: June 12, 2023

Published: June 30, 2023

Keywords:

Ezetimibe, spinal cord injury, inflammation, oxidative stress, AMPK/Nrf2 pathway

ABSTRACT

Sustained inflammation after a traumatic spinal cord injury (TSCI) triggers oxidative stress and neuronal apoptosis, hindering functional recovery. Ezetimibe (EZE) has been reported to have anti-inflammatory and antioxidative properties in hepatology-related diseases, but its potential role in SCI remains unclear. In this study, we evaluated the therapeutic effect of EZE on inflammatory microglia and in an SCI model and elucidated the underlying mechanism. First, we stimulated the BV2 microglia cell line with LPS, and we also induced moderate spinal cord injuries in adult male C57BL/6 mice. Both the cells and mice were treated with EZE, and we investigated inflammation, oxidative stress, neurologic damage, and motor function in vitro and in vivo, respectively. Our findings demonstrated that EZE administration attenuates inflammation in microglia by regulating the AMPK/Nrf2 axis. Furthermore, EZE treatment reduced inflammation and oxidative stress levels in the injured spinal cord. Additionally, treatment with EZE decreased glial scarring and improved motor function recovery, indicating the protective role of EZE in SCI. EZE was found to have anti-inflammatory and antioxidative effects on SCI, and it modulated the AMPK/Nrf2 pathway in microglia. Moreover, EZE prevented histological destruction of the spinal cord tissue. In conclusion, EZE shows promise as a drug to protect neurologic integrity following post-SCI.

Doi: <http://dx.doi.org/10.14715/cmb/2023.69.6.26>

Copyright: © 2023 by the C.M.B. Association. All rights reserved.

Introduction

Traumatic spinal cord injury (TSCI) is a deteriorative neurological symptom characterized as decrudescence of sensorimotor function and disorder of the autonomic nervous system, sometimes causing death in danger (1). Primary injury caused by trauma is traditionally considered to be incurable, whereas secondary injury associated with a series of organic stress responses including neuroinflammation, oxidative stress and apoptosis remains the underlying therapeutic research focus (2,3). Following trauma, damaged neural cells immediately induce neuroinflammation that activates microglia in situ and summons accumulation of glial groups surrounding the injury center (4,5). Besides, peripheric pro-inflammatory clusters, such as granulocyte, monocyte and even erythrocyte, traverse into the epicenter resulting from disruption of the blood-spinal cord barrier (BSCB) and rupture of micro-vessel (6,7). The increasing level of neuroinflammation and the majority of damaged neurons generate massive reactive oxygen species (ROS) and neurotoxic substances, causing subsequent neuron death (8). Hence, the critical issue with the improvement of neural protection is the modulation of neuroinflammation levels and reduction of oxidative stress. Ezetimibe (EZE) is a novel antilipemic agent via inhibition of Niemann-Pick disease type C1-like 1- (NPC1L1-) induced cholesterol absorption (9). Recent studies show that EZE has pleiotropic properties independent of NPC1L1- in neurology (10,11). For instance, EZE has reported an improved effect of middle cerebral artery occlusion (MCAO) via attenuation of neuronal apoptosis and activation of autophagy (12). Moreover, in an Alzheimer model, Yu and his colleagues reported EZE administration alleviated dementia-induced memory dysfunction.¹⁰ Notably, EZE mitigated adverse symptoms of acute stroke progression in a randomized and controlled clinical study (13). Adenosine monophosphate-activated protein kinase (AMPK) activation promotes the initiation of nuclear factor erythroid 2-related factor 2 (Nrf2), which reduces ROS via an increase of heme oxygenase 1(HO-1) (14,15). Also, Nrf2 decreases proinflammatory cytokines (16). In hepatocytes, the anti-inflammatory specialty of EZE relied on AMPK induction (17). Therefore, EZE may exert its neuroprotective effects through the activation of AMPK/Nrf2. In the current study, we hypothesized the protective effects of EZE in the SCI model via attenuating oxidative stress and neuroinflammation via the AMPK/Nrf2 pathway.

Materials and Methods

Materials and Methods

Microglia treatment

BV2 microglia line was purchased from American Type Culture Collection (ATCC) (Manassas, VA, USA) and seeded into 25 cm² flask with dulbecco's modified eagle medium (DMEM, Gibco, Rockville, MD, USA) supplemented 10% fetal bovine serum (FBS, Gibco, Rockville, MD, USA) and 1% Penicillin/ Streptomycin (Gibco, Rockville, MD, USA). The cells were randomly assigned to four different experimental groups. NC group, LPS

* Corresponding author. Email: qiongyacc@126.com

group and LPS+ 50 nM EZE group, as well as LPS+ 100 nM EZE group, were established. When cell confluence reached 90%, the complete medium was replaced by an FBS-free medium for 24 h at 37°C, then medium with EZE (50 nM and 100 nM, APExBIO, Houston, TX, USA) in dimethylsulfoxide (DMSO) was treated with BV2 cells for 24 h. Then, LPS (1 µg/mL, Sigma, St. Louis, MO, USA) was employed to activate BV2 cells inflammation for 16 h.

Animals and modeling

Adult female C57/B6J mice (20-22 g, 6-8 weeks) were obtained from Beijing Vital River Laboratory Animal Technology Co., Ltd. (Beijing, China) and housed in Tsinghua University Animal Center. All animal operations were approved by the Animal Ethics Committee of Tsinghua University Animal Center and the SCI modeling procedure. The mice were randomly assigned to three different experimental groups. The Sham group, SCI group and SCI+EZE group were established in the study. For SCI modeling, we anesthetized mice using 1% pentobarbital sodium (50 mg/kg, I.P.). Then mice were exposed to the T10 spinal cord and 60 kilodyne causes cord trauma (Sham only performed laminectomy). Immediately, EZE (500 µg/kg, every 5 min at a time, total 4 times) dissolved by 10% DMSO was employed using intranasal administration.

Quantitative reverse transcription-polymerase chain reaction (qRT-PCR)

Total RNA was extracted from cord tissue using a Total RNA Extraction Reagent (YiFeiXue Biotechnology, Nanjing, China) following the manufacturer's protocol. Reverse transcription was conducted for cDNA synthesis using a qScript Flex cDNA Synthesis Kit (Quanta Biosciences, Shanghai, USA). Quantitative analysis was performed using Perfecta SYBR Green Supermix (Quanta Biosciences, Shanghai, USA). The analysis of the melting curve was employed to determine the RNA level of interest. GAPDH was employed for normalization. The data of mRNA expression levels were quantified by the $2^{-\Delta\Delta Ct}$ methods. Our used primers of RNAs are listed in Table 1.

Western blot

Cells were harvested using a Total Protein Extraction Kit (KeyGEN, Nanjing, China) according to the manu-

facturer's protocol. Protein quantification was performed using a Bicinchoninic acid method (Beyotime, Shanghai, China). Western blot was carried out using a 10% sodium dodecyl sulfate-polyacrylamide gel electrophoresis (SDS-PAGE). The antibodies in our study included p-AMAK (1;1000, Abcam, Cambridge, MA, USA), AMAK (1;1000, Abcam, Cambridge, MA, USA), Nrf2 (1:1000, Abcam, Cambridge, MA, USA), GAPDH (1:2000, Abcam, Cambridge, MA, USA), Goat Anti-Rabbit IgG H&L (HRP) (1:2000, Abcam, Cambridge, MA, USA). Band images were exhibited using an enhanced chemiluminescence (ECL) system.

MDA and ROS measurement

Spinal cord homogenate was centrifuged and the supernatant was collected for MDA assay by following the manufacturer's instructions (Keygen, Nanjing, China). After incubating with the reagent and boiling for 50 min, the sample was placed on ice for rapid cooling. The supernatant was detected at 532 nm following centrifugation. For ROS, we used a ROS Assay Kit (Beyotime, Shanghai, China) directed by the manufacturer's protocol. Collected cells from tissue were resuspended in DCFH-DA diluted in DMEM. After a complete reaction with the probe, ROS was measured in the condition that 488 nm excitation wavelength and 2 and 532 nm emission wavelength using a spectrophotometer.

Immunofluorescence and immunohistochemical staining (IF and IHC)

Tissue was fixated with 4% paraformaldehyde (PFA) and conducted dehydration through different gradients of alcohol. Then the tissue was embedded into the paraffin and cut into sections (5 µm) using a rotary microtome. Sections were incubated with primary antibodies IBA-1 (Abcam, Cambridge, MA, USA, 1:500), CD11c (Abcam, Cambridge, MA, USA, 1:200), NF-κB (Abcam, Cambridge, MA, USA, 1:200) overnight. For IF, Alexa Fluor® coupled secondary antibodies (Invitrogen, Carlsbad, CA, USA, 1:200) were conducted with sections. For IHC, we used an Immunochromogenic Reagent (Gene Tech, Shanghai, China) by following the manufacturer's protocol. The nucleus was stained with diamidine phenyl indole (DAPI) for IF or hematoxylin for IHC. Then the images of sections were visualized and collected using a microscope.

Table 1. Primer sequences of quantitative reverse transcription-polymerase chain reaction.

Oligo Name		Sequence (5' -----> 3')
TNF-α	Forward	CTGAACTTCGGGGTGATCGG
	Reverse	GGCTTGTCACCTCGAATTTTGAG
IL-6	Forward	TCTATACCACTTCACAAGTCGGA
	Reverse	GAATTGCCATTGCACAACCTCTTT
IL-1β	Forward	CTGTGACTCATGGGATGATGATG
	Reverse	CGGAGCCTGTAGTGCAGTTG
GAPDH	Forward	TGACCTCAACTACATGGTCTACA
	Reverse	CTTCCCATTTCTCGGCCTTG
Nrf2	Forward	CTTTAGTCAGCGACAGAAGGAC
	Reverse	AGGCATCTTGTGGGAATGTG
HO-1	Forward	AGGTACACATCCAAGCCGAGA
	Reverse	CATCACCAGCTTAAAGCCTTCT

Enzyme-linked immunosorbent assay (ELISA)

Mouse spinal cords were collected at 1-day post-trauma. We centrifuged the homogenate for 10 minutes and collected the supernatant. ELISA was conducted using ELISA Kits (Beyotime, Shanghai, China) according to the manufacturer's instructions. The OD value of samples was measured at 450 nm using a multiscan spectrum.

Basso mouse scale behavioral evaluation

Each mouse was observed free movement in the open field for 4 minutes at 1, 3, 7, 14, and 28 days following trauma, respectively. Two blind researchers were employed to assess the locomotor function of mice with BMS.

Statistical analysis

Data were obtained from the study and exhibited as the means \pm SD (standard deviation). The difference between the two groups in statistics was assessed with Student's t-test. The difference in more than two groups was evaluated using ANOVA. Data were collected and analyzed using Statistical Product and Service Solutions (SPSS) 18.0 software (Chicago, IL, USA). $P < 0.05$ is identified as statistical significance.

Results

EZE administration inhibits microglial activation via regulation of the AMPK/Nrf2 axis

To verify whether EZE inhibits microglial activation and the underlying mechanism, we examined CD11c expression, a classical biomarker of pro-inflammatory microglia, and ionized calcium binding adaptor molecule-1 (IBA-1) using IF following EZE treatment or not. The result exhibited a remarkable increase of CD11c expression in the LPS group whereas a decrease in CD11c level after EZE employment in IBA1-positive microglia (Figure 1A). Besides, we further detected the level of nuclear factor- κ B (NF- κ B), showing a significant elevation of NF- κ B in LPS-activated microglia. However, we witnessed a decreased expression of NF- κ B with EZE administration compared with the LPS group (Figure 1B). The activation of the AMPK/Nrf2 pathway has been demonstrated as an inhibition of NF- κ B, we thereby investigated the influence of EZE to the AMPK/Nrf2 pathway. Western blot exhibited that LPS increased AMPK but decreased Nrf2 expression, however, EZE treatment markedly increased AMPK and Nrf2 expressions compared with the LPS group (Figure 1C-E), indicating that EZE utilization suppressed LPS-induced microglial activation via positively regulating AMPK/Nrf2 axis.

The anti-inflammatory effect of EZE in LPS-induced microglia

Next, we explored the affection of EZE to microglial inflammation, the classical pro-inflammatory cytokines including tumor necrosis factor- α (TNF- α), interleukin-1beta (IL-1 β) and IL-6 were measured using qRT-PCR, showing a prominent increase of the classical pro-inflammatory cytokines RNAs following LPS stimuli. Inversely, EZE treatment remarkably reduced the RNA levels of TNF- α , IL-1 β and IL-6 in activated microglia (Figure 2A-2C). Furtherly, we conduct ELISA for medium supernatant to examine the levels of TNF- α , IL-1 β and IL-6 (Fi-

gure 2D-2F). The results showed the ELISA in consistent with the RNA levels, indicating the anti-proinflammatory effect of EZE in activated microglia.

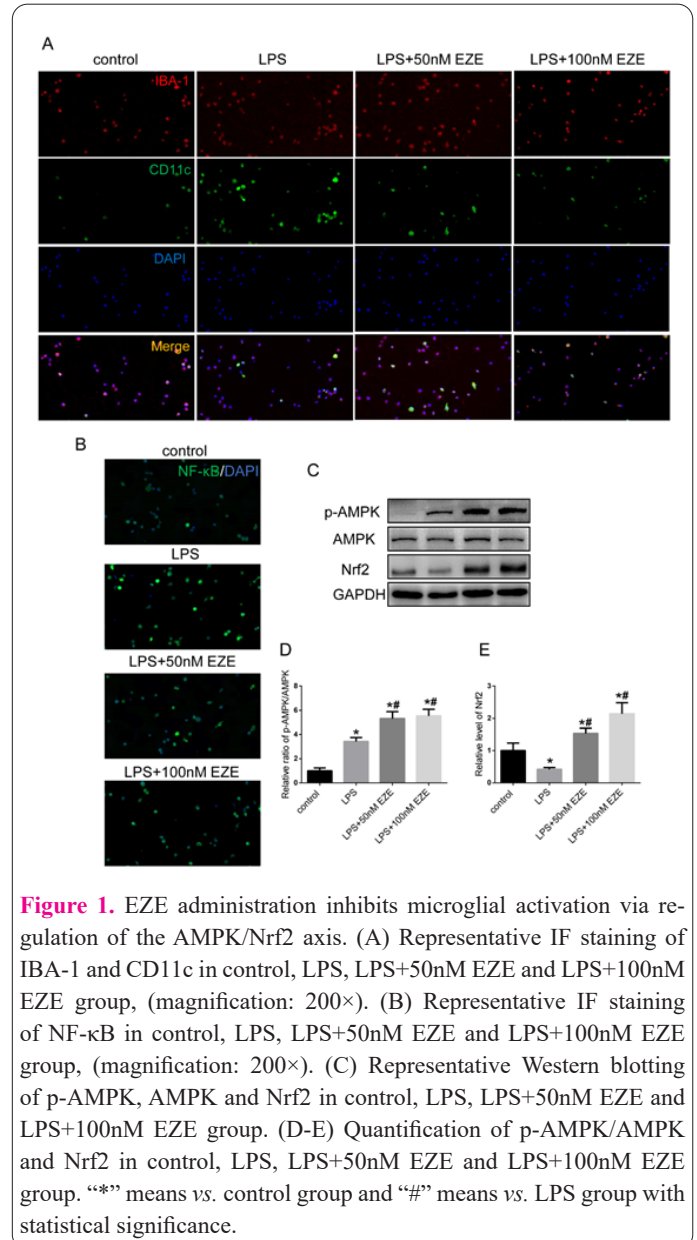


Figure 1. EZE administration inhibits microglial activation via regulation of the AMPK/Nrf2 axis. (A) Representative IF staining of IBA-1 and CD11c in control, LPS, LPS+50nM EZE and LPS+100nM EZE group, (magnification: 200 \times). (B) Representative IF staining of NF- κ B in control, LPS, LPS+50nM EZE and LPS+100nM EZE group, (magnification: 200 \times). (C) Representative Western blotting of p-AMPK, AMPK and Nrf2 in control, LPS, LPS+50nM EZE and LPS+100nM EZE group. (D-E) Quantification of p-AMPK/AMPK and Nrf2 in control, LPS, LPS+50nM EZE and LPS+100nM EZE group. “*” means vs. control group and “#” means vs. LPS group with statistical significance.

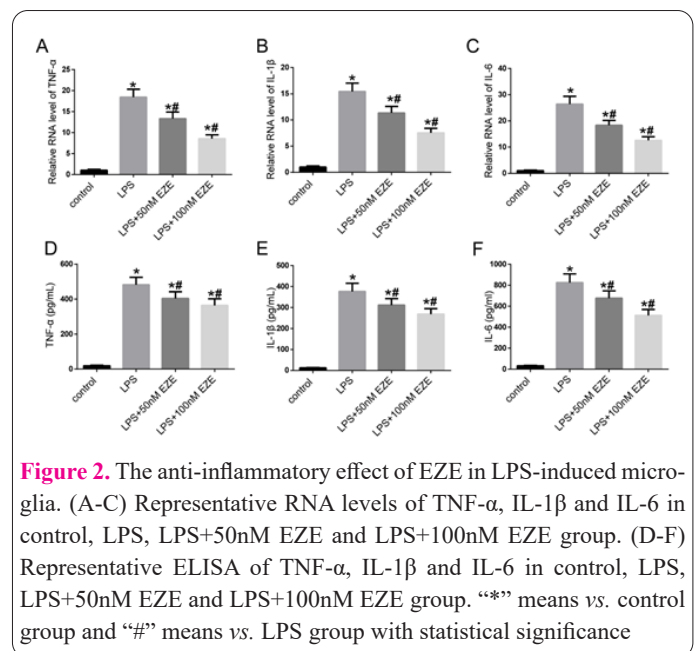


Figure 2. The anti-inflammatory effect of EZE in LPS-induced microglia. (A-C) Representative RNA levels of TNF- α , IL-1 β and IL-6 in control, LPS, LPS+50nM EZE and LPS+100nM EZE group. (D-F) Representative ELISA of TNF- α , IL-1 β and IL-6 in control, LPS, LPS+50nM EZE and LPS+100nM EZE group. “*” means vs. control group and “#” means vs. LPS group with statistical significance.

Administration of EZE mitigates neuroinflammation following SCI trauma

We next evaluated the neuroinflammation level after SCI in vivo. To verify the level of activated microglia in the injured site, we detected the CD11c and IBA1 expressions on days 3 post-trauma using IF. The images displayed CD11c and IBA1 double-positive cells increased significantly in the injured site following SCI, however, administration of EZE reduced the number of CD11c and IBA1 double-positive cells in the center of injury (Figure 3A). It was implied that EZE treatment alleviated microglial activation in the injured spinal cord. Moreover, ELISA showed that EZE treatment significantly decreased the inflammatory indexes TNF- α , IL-1 β and IL-6 levels in the injured spinal cord on days 3 post-SCI (Figure 3B-3D). Moreover, we detected p-AMPK expression in the spinal cord using IHC, finding that EZE employment markedly increased p-AMPK expression in the injured site compared with the SCI group on days 3 post-SCI (Figure 3E). Hence, we certified that EZE administration decreased neuroinflammation in the acute period of SCI.

EZE treatment decreases ROS and lipid oxidation in injured spinal cord

Neuroinflammation associates with the occurrence of oxidative stress in neural tissue. To investigate the effect of EZE in SCI-induced oxidative stress, we first detected the ROS level in injured tissues. The results showed that massive ROS following SCI was mitigated by EZE treatment (Figure 4A). Besides, the RNA levels of Nrf2 and hemoxygenase-1 (HO-1) increased in the injury cord after EZE administration (Figure 4B&4C). Further, we measured the malondialdehyde level, a metabolite of oxidized lipids, in the injured cord, finding that EZE reduced remarkably the excessive level of MDA after SCI (Figure 4D). Hence, EZE treatment elevated the motor score according to BMS after the acute phase of SCI (Figure 4E).

Discussion

In the current study, we demonstrated that EZE attenuated oxidative stress and neuroinflammation after SCI in mice. Moreover, we observed that EZE increased endogenous AMPK/Nrf2 axis in activated microglia and administration of EZE improved motor functional recovery after SCI. Through inhibition of microglial activation, EZE decreased the expressions of inflammatory cytokines. EZE treatment also mitigated the level of oxidative stress resulting from a decrease of ROS and elevation of Nrf2 and HO-1. Taken together, the outcomes contribute to a beneficial function of neurobehavioral recovery. Neuroinflammation response associated with oxidative stress is a critical process aggravating neural destruction after SCI (18). Inflammatory cascades cause destructive and extensive secondary injury, inducing glial hyperplasia, demyelination, and neuronal death. EZE, a new lipid-lowering drug, is shown as a promising antioxidant and anti-inflammation in various neurological diseases (19,20). Increasing studies (21,22) have demonstrated the potential improvement of EZE in ischemic-related oxidative stress and inflammation. In a clinical study, EZE was reported to ameliorate exacerbation of neurologic cognition and volume of cerebral areas in stroke after atrial fibrillation. In addition, Yu et al. verified that EZE attenuated oxidative

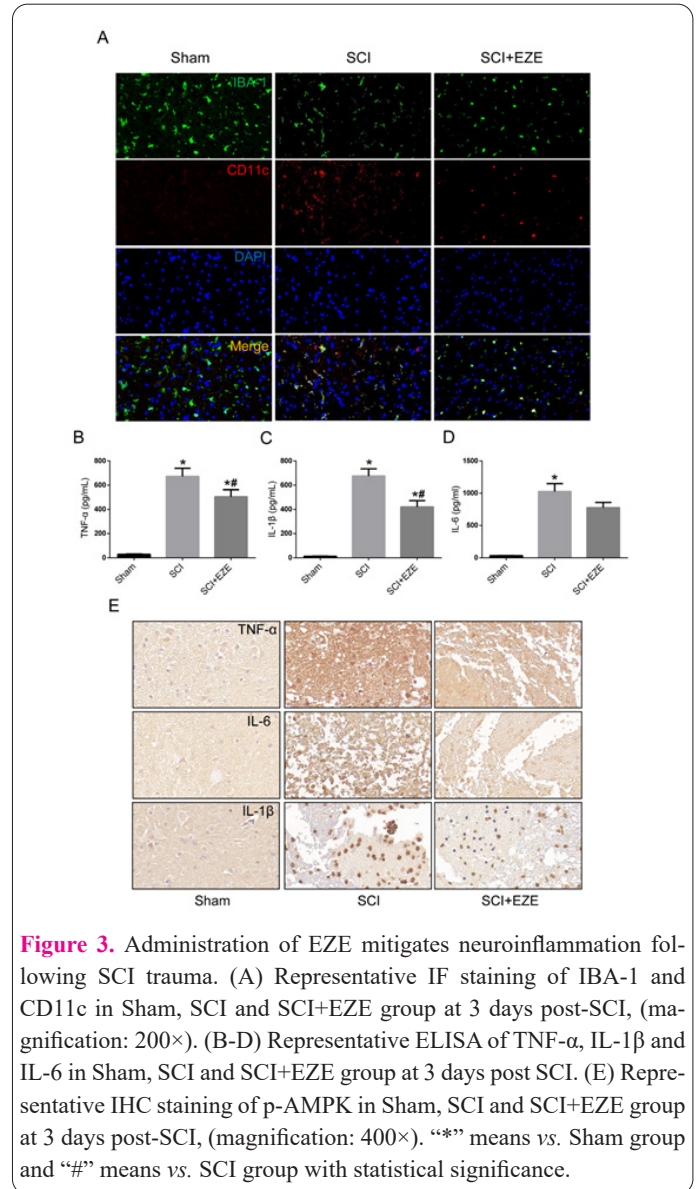


Figure 3. Administration of EZE mitigates neuroinflammation following SCI trauma. (A) Representative IF staining of IBA-1 and CD11c in Sham, SCI and SCI+EZE group at 3 days post-SCI, (magnification: 200 \times). (B-D) Representative ELISA of TNF- α , IL-1 β and IL-6 in Sham, SCI and SCI+EZE group at 3 days post SCI. (E) Representative IHC staining of p-AMPK in Sham, SCI and SCI+EZE group at 3 days post-SCI, (magnification: 400 \times). “*” means vs. Sham group and “#” means vs. SCI group with statistical significance.

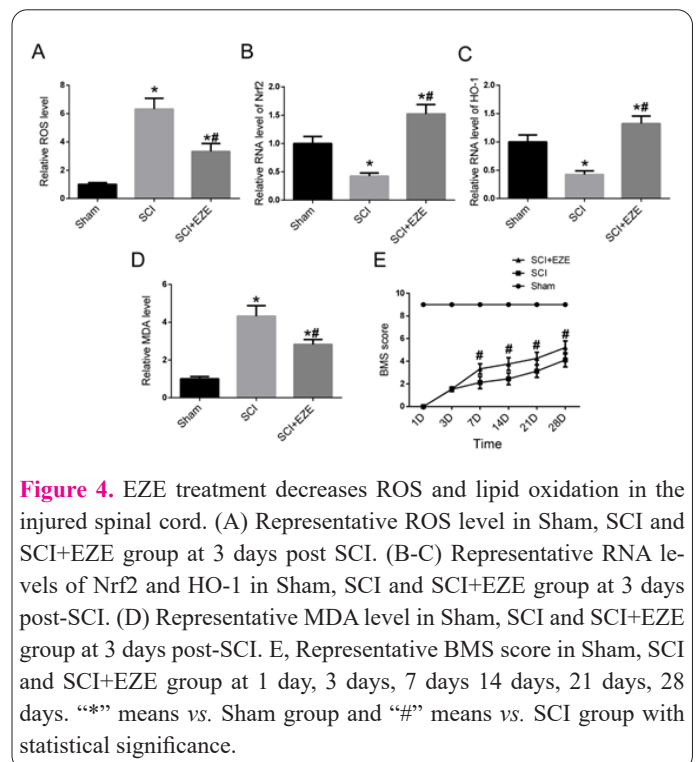


Figure 4. EZE treatment decreases ROS and lipid oxidation in the injured spinal cord. (A) Representative ROS level in Sham, SCI and SCI+EZE group at 3 days post SCI. (B-C) Representative RNA levels of Nrf2 and HO-1 in Sham, SCI and SCI+EZE group at 3 days post-SCI. (D) Representative MDA level in Sham, SCI and SCI+EZE group at 3 days post-SCI. (E) Representative BMS score in Sham, SCI and SCI+EZE group at 1 day, 3 days, 7 days 14 days, 21 days, 28 days. “*” means vs. Sham group and “#” means vs. SCI group with statistical significance.

stress and neuroinflammation after MCAO in rats (20). According to these discoveries, we attempted to explore the effect of EZE in SCI and proved that administration of EZE reduced the loss of motor function, microglial activation, inflammatory factors release, and ROS and MDA levels. Specifically, treatment with EZE inhibited microglia-induced neuroinflammation via regulating AMPK/Nrf2 pathway. Hence, we witnessed a significant improvement in BMS scores in mice treated with EZE after the acute phase of SCI. Evidences (22,23) showed that EZE increased oxygen consumption and enhanced ADP generation, causing the increase of ADP/ATP ratio and then activating AMPK. Our findings verified that the endogenous p-AMPK expression increased both in activated microglia and injured spinal cord, EZE treatment further increased p-AMPK level. Moreover, we found increased expressions of Nrf2 and HO-1 after EZE utilization in SCI mice. These findings further confirmed the antioxidant stress effect of EZE. Besides, due to the elevation of p-AMPK, the microglial inflammation was reduced both in vitro and in vivo, indicating that EZE exerts an anti-inflammatory effect depending on p-AMPK increase. The novelty of the present study is that we first demonstrated the potential anti-inflammatory and anti-oxidative stress effects of EZE and confirmed the positive ameliorative function of EZE treatment after SCI. However, there were some limitations in the research. We did not completely exclude the possibility of other pathways that inhibit the NF- κ B pathway. Therefore, more works need to concentrate on the correlation of other NF- κ B activators. Besides, we only assessed the one-time window target for microglial inflammation with EZE treatment, alternative cellular processing in other cell groups (e.g., Neuron) associated with SCI will need to be investigated. Last, for the regulation of the AMPK pathway, EZE was previously reported to attenuate apoptosis via AMPK-induced autophagy in neurology. In our study, we also witnessed decreased neuroinflammation and oxidative stress via activation of the AMPK/Nrf2 pathway. Hence, we speculated that EZE may exert an anti-apoptosis function in damaged neurons via activating AMPK downstream targets. Taken together, subsequent studies are urgent to be complemented to better illuminate the full therapeutic effect of EZE.

In summary, the study proves that EZE treatment reduces microglial inflammation by regulating of AMPK/NF- κ B pathway in vitro. Moreover, Treatment with EZE reduced neuroinflammation and oxidative stress via AMPK/Nrf2 pathway in SCI mice.

Therefore, EZE improves motor functional recovery and is proven to be a promising agent for neural protection after SCI.

Conflict of Interests

The authors declared no conflict of interest.

References

- Ahuja CS, Wilson JR, Nori S, et al. Traumatic spinal cord injury. *Nat Rev Dis Primers* 2017; 3: 17018.
- Shank CD, Walters BC, Hadley MN. Current Topics in the Management of Acute Traumatic Spinal Cord Injury. *Neurocrit Care* 2019; 30(2): 261-271.
- David G, Mohammadi S, Martin AR, et al. Traumatic and nontraumatic spinal cord injury: pathological insights from neuroimaging. *Nat Rev Neurol* 2019; 15(12): 718-731.
- Goins J, Henkel N, Coulibaly AP, Isaacson LG. Activated Microglia in the Rat Spinal Cord Following Peripheral Axon Injury Promote Glial and Neuronal Plasticity Which is Necessary for Long-Term Neuronal Survival. *Cell Mol Neurobiol* 2021; 41(2): 309-326.
- Wang C, Wang Q, Lou Y, et al. Salidroside attenuates neuroinflammation and improves functional recovery after spinal cord injury through microglia polarization regulation. *J Cell Mol Med* 2018; 22(2): 1148-1166.
- Park CS, Lee JY, Choi HY, Ju BG, Youn I, Yune TY. Protocatechuic acid improves functional recovery after spinal cord injury by attenuating blood-spinal cord barrier disruption and hemorrhage in rats. *Neurochem Int* 2019; 124: 181-192.
- Sahib S, Niu F, Sharma A, et al. Potentiation of spinal cord conduction and neuroprotection following nanodelivery of DL-3-n-butylphthalide in titanium implanted nanomaterial in a focal spinal cord injury induced functional outcome, blood-spinal cord barrier breakdown and edema formation. *Int Rev Neurobiol* 2019; 146: 153-188.
- Zhang B, Bailey WM, McVicar AL, Gensel JC. Age increases reactive oxygen species production in macrophages and potentiates oxidative damage after spinal cord injury. *Neurobiol Aging* 2016; 47: 157-167.
- Ge L, Wang J, Qi W, et al. The cholesterol absorption inhibitor ezetimibe acts by blocking the sterol-induced internalization of NPC1L1. *Cell Metab* 2008; 7(6): 508-519.
- Dalla Y, Singh N, Jaggi AS, Singh D, Ghulati P. Potential of ezetimibe in memory deficits associated with dementia of Alzheimer's type in mice. *Indian J Pharmacol* 2009; 41(6): 262-267.
- Liu CH, Chen TH, Lin MS, et al. Ezetimibe-Simvastatin Therapy Reduce Recurrent Ischemic Stroke Risks in Type 2 Diabetic Patients. *J Clin Endocr Metab* 2016; 101(8): 2994-3001.
- Yu J, Li X, Matei N, et al. Ezetimibe, a NPC1L1 inhibitor, attenuates neuronal apoptosis through AMPK dependent autophagy activation after MCAO in rats. *Exp Neurol* 2018; 307: 12-23.
- Yang L, Zhao P, Zhao J, Wang J, Shi L, Wang X. Effects of ezetimibe and anticoagulant combined therapy on progressing stroke: a randomized, placebo-controlled study. *J Neurol* 2016; 263(12): 2438-2445.
- Al-Kuraishy HM, Al-Gareeb AI, Al-Maiahy TJ, Alexiou A, Mukerjee N, Batiha GE. Prostaglandins and non-steroidal anti-inflammatory drugs in Covid-19. *Biotechnol Genet Eng* 2022: 1-21.
- Peng M, Qiang L, Xu Y, Li C, Li T, Wang J. Inhibition of JNK and activation of the AMPK-Nrf2 axis by corosolic acid suppress osteolysis and oxidative stress. *Nitric Oxide-Biol Ch* 2019; 82: 12-24.
- Permpoonputtana K, Govitrapong P. The anti-inflammatory effect of melatonin on methamphetamine-induced proinflammatory mediators in human neuroblastoma dopamine SH-SY5Y cell lines. *Neurotox Res* 2013; 23(2): 189-199.
- Kim SH, Kim G, Han DH, et al. Ezetimibe ameliorates steatohepatitis via AMP activated protein kinase-TFEB-mediated activation of autophagy and NLRP3 inflammasome inhibition. *Autophagy* 2017; 13(10): 1767-1781.
- Zhou J, Li Z, Wu T, Zhao Q, Zhao Q, Cao Y. LncGBP9/miR-34a axis drives macrophages toward a phenotype conducive for spinal cord injury repair via STAT1/STAT6 and SOCS3. *J Neuroinflamm* 2020; 17(1): 134.
- Trocha M, Merwid-Lad A, Chlebda E, et al. Influence of ezetimibe on selected parameters of oxidative stress in rat liver subjected to ischemia/reperfusion. *Arch Med Sci* 2014; 10(4): 817-824.
- N PD, Kondengadan MS, Sweilam SH, et al. Neuroprotective role of coconut oil for the prevention and treatment of Parkinson's

- disease: potential mechanisms of action. *Biotechnol Genet Eng* 2022; 1-33.
21. Peserico D, Stranieri C, Garbin U, et al. Ezetimibe Prevents Ischemia/Reperfusion-Induced Oxidative Stress and Up-Regulates Nrf2/ARE and UPR Signaling Pathways. *Antioxidants-Basel* 2020; 9(4): 349.
22. Lee DH, Han DH, Nam KT, et al. Ezetimibe, an NPC1L1 inhibitor, is a potent Nrf2 activator that protects mice from diet-induced nonalcoholic steatohepatitis. *Free Radical Bio Med* 2016; 99: 520-532.
23. Hernandez-Mijares A, Banuls C, Rovira-Llopis S, et al. Effects of simvastatin, ezetimibe and simvastatin/ezetimibe on mitochondrial function and leukocyte/endothelial cell interactions in patients with hypercholesterolemia. *Atherosclerosis* 2016; 247: 40-47.